

Article

# LUCA: A Sentinel-1 SAR-Based Global Forest Land Use Change Alert

Adugna Mullissa <sup>1,2,\*</sup>, Sasan Saatchi <sup>1,2,3</sup>, Ricardo Dalagnol <sup>1,2,3</sup>, Tyler Erickson <sup>4</sup>, Naomi Provost <sup>1</sup>, Fiona Osborn <sup>1</sup>, Aleena Ashary <sup>1</sup>, Violet Moon <sup>1</sup> and Daniel Melling <sup>1</sup>

<sup>1</sup> Ctrees.org, Pasadena, CA 91105, USA

<sup>2</sup> Institute of Environment and Sustainability, University of California, Los Angeles, CA 90095, USA

<sup>3</sup> Jet Propulsion Laboratory, California Institute of Technology, Pasadena, CA 91109, USA

<sup>4</sup> VorGeo, Los Altos, CA 94022, USA

\* Correspondence: amullissa@ctrees.org

**Abstract:** The Land Use Change Alert (LUCA) dataset was developed for effective and timely monitoring of global forest changes that are mostly associated with human activities. Near-real-time changes of forest land use are mapped at 0.05 ha minimum mapping unit for all forest types across the Earth's ecoregions, every two weeks. LUCA is based on Sentinel-1 cloud penetrating synthetic aperture radar (SAR) observations to circumvent limitations of optical imagery from pervasive cloud cover over forested areas globally, and especially in the tropics. The methodology is based on a combination of time-series change detection and machine learning analytics to achieve high accuracy of alerts across all ecoregions and landscapes globally with an average area-adjusted users and producers accuracy of 83% and 63%, respectively. The bi-weekly global alert maps capture forest clearing associated with deforestation and industrial timber harvesting, along with forest degradation associated with selective logging, fragmentation, fire, and roads. The product was developed and released publicly through Google Earth Engine to allow for the rapid assessment of land use change activities, quantifying patterns and processes driving forest change and dynamics across forest ecoregions. LUCA is designed to help monitor a variety of emission reduction programs at the local to regional scales and play a key role in implementing regulations on deforestation-free products.



**Citation:** Mullissa, A.; Saatchi, S.; Dalagnol, R.; Erickson, T.; Provost, N.; Osborn, F.; Ashary, A.; Moon, V.; Melling, D. LUCA: A Sentinel-1 SAR-Based Global Forest Land Use Change Alert. *Remote Sens.* **2024**, *16*, 2151. <https://doi.org/10.3390/rs16122151>

Academic Editor: Michael Sprintsin

Received: 8 April 2024

Revised: 27 May 2024

Accepted: 6 June 2024

Published: 13 June 2024



**Copyright:** © 2024 by the authors. Licensee MDPI, Basel, Switzerland. This article is an open access article distributed under the terms and conditions of the Creative Commons Attribution (CC BY) license (<https://creativecommons.org/licenses/by/4.0/>).

## 1. Background & Summary

Forest changes driven by land use activities associated with the expansion of grazing and agricultural land and timber harvest for fuels and wood products are the critical drivers of the global economy, a significant source of carbon emissions, and the main cause of habitat fragmentation, carbon emissions, and other negative environmental impacts [1]. The conversion of natural forests to other land uses has major impacts on the terrestrial carbon cycle, biodiversity, and livelihood of forest communities, as well as other ecosystem services such as water and energy [2–4]. In recent years, nation states under the Paris Agreement [5] and a large number of private companies and public-private coalitions have made commitments to reducing emissions from deforestation and degradation (REDD+) and to participating in a variety of carbon offset programs and regulations [6]. Although these regulations are currently focused on tropical deforestation, future climate mitigation policies to reduce carbon emissions from land use changes and the focus on nature-based solutions will eventually extend these regulations to cover entire global biomes, covering both domestic and export markets and supply chains [7]. Near-real-time monitoring of changes of forest land use, therefore, can contribute to implementing and enforcing these regulations and provide reliable data for timely interventions. Currently, several alert systems function at the local or regional levels through remote sensing data and optical and microwave satellite observations [8–12]. These alert systems have two distinct functions for

being used either as an early warning system to inform strategic and effective environmental responses and for the systematic evaluation of the outcomes of environmental interventions, impacts, and progress. Furthermore, by delivering time-sensitive information to decision makers and practitioners who use measures to reduce ecosystem destruction, the alert systems can support a variety of local and regional operational actions [13].

Remote sensing alert systems have improved substantially in recent years due to the availability of analysis-ready and calibrated satellite data in the cloud, machine learning algorithms, and AI-enabled analytics for big data processing. A few notable online platforms for detecting and tracking deforestation and for performing ad hoc analysis on a web-based platforms are Prodes [14], a deforestation tracking tool in the Brazilian Amazon developed by the Brazilian Instituto Nacional de Pesquisas Espaciais (INPE); a platform created by the global forest watch [15]; and the new online platform launched by Brazilian MapBiomass in 2023 to map deforestation in Brazil (<https://alerta.mapbiomas.org/>, accessed on: 5 January 2024).

These platforms typically constitute a near-real-time forest land use change dataset usually derived from optical satellite data and a front end web application that allows ad hoc requests for extraction and analysis of user requests. However, traditional optical sensor sensitivity to cloud cover limits its applicability in regions with pervasive cloud cover throughout the year. The advent of synthetic aperture radar (SAR) sensors was a game changer, as it allowed for the acquisition of images in almost all weather, enabling the detection of forest change in almost the same time as it occurs [12]. The launch of the Sentinel-1 satellites and the associated open data policy have been critical for the proliferation of near-real-time forest cover change monitoring via the use of a dense stack of cloud-penetrating radar images [8]. A few examples of radar-based near-real-time forest disturbance alerts include the radar for detecting deforestation (RADD) alert system [8] that is based on European Space Agency Sentinel-1 SAR images and operates in the humid tropics in 50 countries world wide. The system developed by French Centre d'Etudes Spatiales de la Biosph're (CESBIO) [16] is another radar-based forest disturbance alert system. DETER-R [17] is another system that uses Sentinel-1 SAR images to detect forest cover change that was designed to complement the Brazilian DETER system. The JJ-FAST alert system developed by the Japanese Space Agency JAXA is based on an ALOS-PALSAR and PALSAR2 ScanSAR data and generates alerts in 75 countries in the tropics [18].

The utilization of Sentinel-1 SAR for global near-real-time forest monitoring covering all forest biomes, however, has been elusive due to radar signal fluctuations induced by seasonal changes in forest phenology, open canopy structure in dry and temperate forests, and snow cover freeze and thaw cycles in boreal forests. Therefore, existing radar-based large-scale forest cover change alert products have rarely ventured out of the humid tropics. In this regard, recent technical and scientific advances in the cloud computing of large remote sensing data [19] coupled with advances in machine learning have opened the door for expanding these near-real-time alerts from the humid tropics to the global scale by enabling the rapid detection of forest land use changes without explicitly mitigating the seasonality in the signal [12]. In this study, we expanded upon these innovations to demonstrate the first-of-its-kind, near-real-time forest land use change alert platform named Land Use Change Alert (LUCA), derived from Sentinel-1 SAR images globally in all forest biomes.

## 2. Methods

The Land Use Change Alert (LUCA) dataset was developed and made freely available at a 10 m pixel size. LUCA was built on Google Earth Engine [19], and forest land use change alerts were first made available starting 1 January 2018 and remain available to the present day at a minimum mapping unit of 0.05 ha. Here, we define forest as areas with a minimum of 15 percent tree cover and an average tree height of 5 m. We selected a 15% threshold to make sure the minimum forest area is equivalent to a Sentinel-1 pixel area, as the forest cover baseline was synthesized from a Landsat image. The main objective for

generating these alerts was to map forest land use changes caused by human activities and understand the drivers for these changes.

The general methodology for generating LUCA is shown in (Figure 1). We first preprocessed the Sentinel-1 images to the analysis-ready data (ARD) level [20]. Secondly, we engineered features to define the statistical properties of stable forest and then synthesized the reference labels and sample training dataset in different forest biomes and trained a machine learning model to derive forest and forest land use change probabilities. The derived forest and forest land use change probabilities were refined in a probabilistic approach [12], and forest land use change alerts were generated. Once the alerts were generated, a post-processing step was applied to remove noisy alerts and provide the final alerts at a minimum mapping unit of 0.05 ha, which are displayed in the online web app.

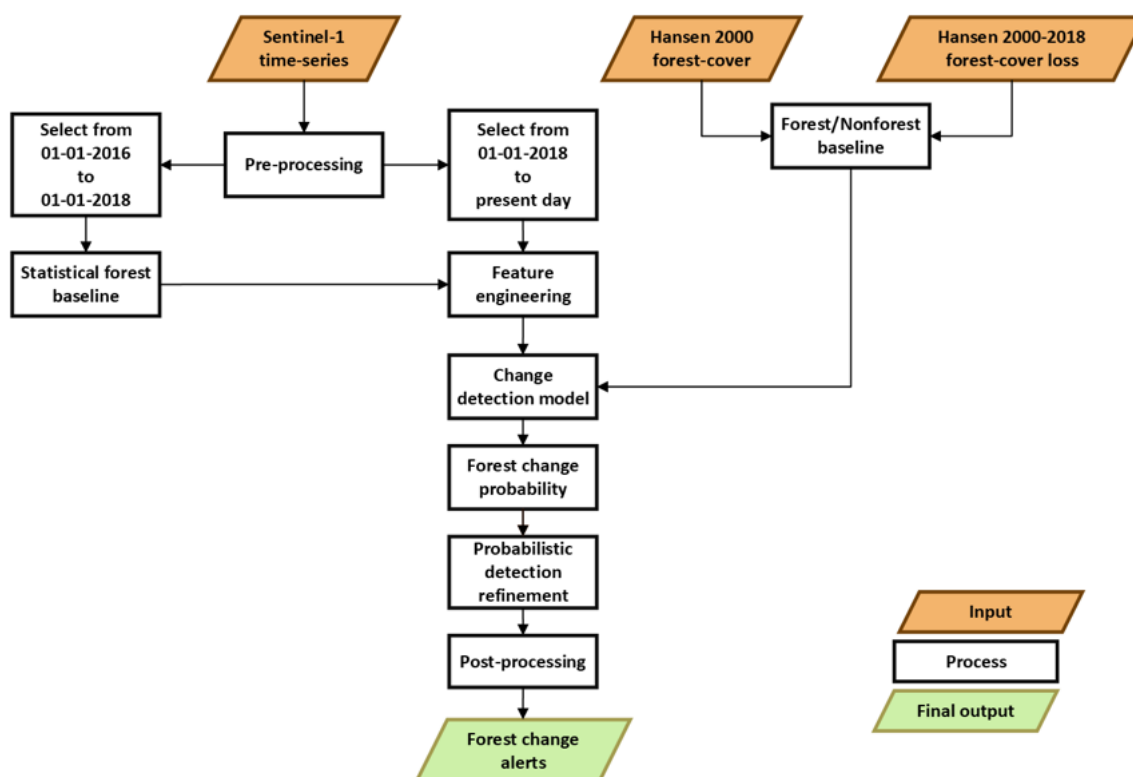


**Figure 1.** The methodological flow chart for LUCA. The historical period is used to create a stable forest baseline of statistical features from 1 January 2016 up to 1 January 2018. Whereas, the monitoring period is used to retroactively detect forest land use change from 1 January 2018 until 15 January 2024.

### 2.1. Sentinel-1 SAR Images

We used a Sentinel-1 SAR ground range detected images in VV and VH polarizations in both ascending and descending orbits covering all major forest biomes globally from 1 January 2016 until 15 January 2024. The Sentinel-1 SAR images were acquired in the interferometric wide swath mode with a resolution of  $5 \times 20$  m in the range and azimuth directions, respectively [21], and were processed for thermal noise removal, calibrated to sigma nought, and corrected for terrain using range Doppler terrain correction with a 10 m pixel size prior to being ingested into Google Earth Engine (GEE).

A total of 883,624 images in the ascending orbit and 974,913 images in the descending orbit were acquired globally between 1 January 2016–15 January 2024 to synthesize features and generate near-real-time forest land use change alerts.

## 2.2. Preprocessing

We created an ARD stack for the Sentinel-1 images in the VV and VH polarization for both the ascending and descending orbits separately. The Sentinel-1 ARD stack was created by applying outlier removal, border noise removal, radiometric terrain normalization, multi-temporal speckle filtering, and image normalization to the Sentinel-1 ground range product available on the GEE data catalog [20]. To that effect, we applied a Hampel filter [22] to remove extreme outliers. We also removed image border noise and artifacts by using the routine suggested in Mullissa et al. 2021 [20]. We applied radiometric terrain flattening by adopting the angular approach suggested by Vollrath et al. 2020, [23] and Hoekmann and Reiche 2015 [24]. We applied a multi-temporal adaptive speckle filtering framework suggested by Quegan and Yu 2001 [25] to reduce speckle prior to applying forest land use change detection algorithms. For quality assurance, we removed images containing rain cells in the tropics and images acquired during the freezing seasons in the northern latitudes prior to applying the forest land use change detection algorithms. We removed images acquired during the snow cover season, as snow significantly decreases the backscattered signal intensity which leads to significant increase in commission error.

## 2.3. Feature Engineering

We split the data into two parts, one being the historical period when the stable forest baseline was established (i.e., 1 January 2016 to 1 January 2018) and the other being the monitoring period when near-real-time alerts were generated (i.e., from 1 January 2018 to 15 January 2024) (Figure 1). To extract the stable forest statistical descriptors, we generated a pixel-wise median and standard deviation of the backscatter values in the stable forest historical period (i.e., 1 January 2016–1 January 2018) for the VV and VH polarizations separately. For the humid tropics, in the absence of seasonality, the best temporal feature to define is the dynamics of the stable forest signal (Figure 2), as it follows a Gaussian distribution and is the median and standard deviation of the signal [8]. The median is preferred to the mean, as it is more robust to outliers. In the dry tropics and temperate regions, the signal is affected by seasonality stemming from change in forest phenology, but in C-band radar such as Sentinel-1, in the leaf off season, there is significant interaction with the branches. Therefore, the seasonality pattern is much smaller than the effect of speckle, so the seasonality is not readily visible without aggregation over an area. In the presence of forest change, the scattering magnitude change in the resolution cell induces a significant decrease in the backscattered signal intensity. The decrease in the backscattered signal is much larger than the decrease in the leaf-off seasons. Therefore, the median and standard deviation remain good descriptors of stable deciduous forest dynamics. The median and standard deviation for both the VV and VH polarization in the historical period defining the stable forest baseline combined with the backscatter images in the monitoring period (i.e., 1 January 2018–15 January 2024) for both the VV and VH polarization sets the change detection configuration in a before-and-after change-detection scenario. In this regard, the applied machine learning algorithms learned to derive the probability of forest and non-forest from every image in the monitoring period as a function of the stable forest median backscatter signal intensities and the standard deviation of the backscatter signal intensity in the historical period.

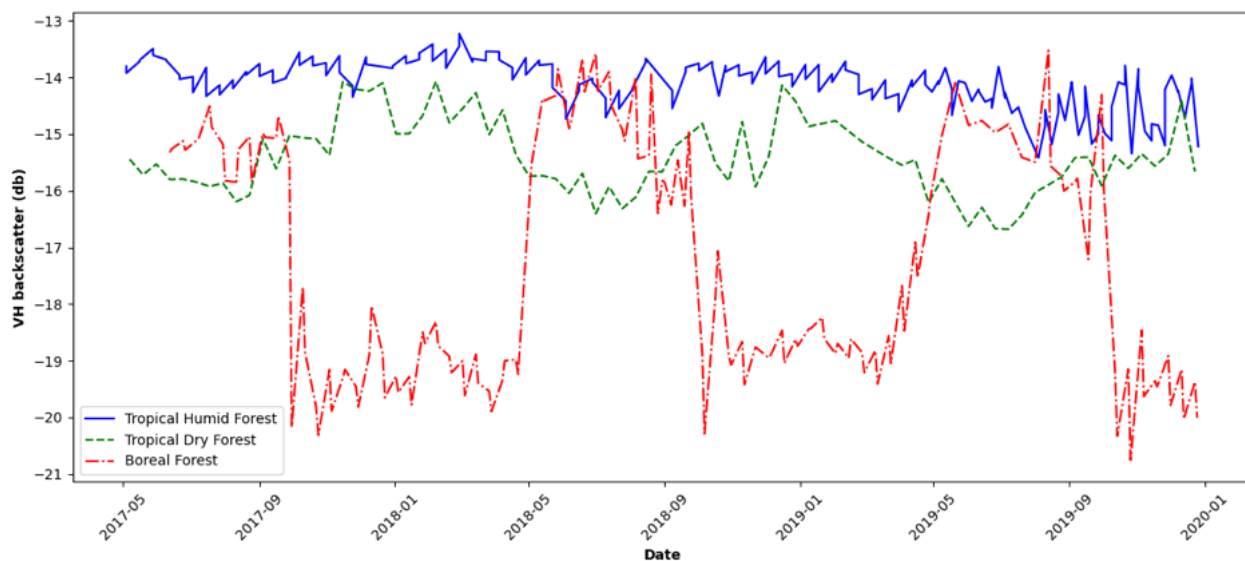


**Figure 2.** The Sentinel-1 SAR backscatter time-series for different forest types. The tropical humid forests (shown in blue) do not show seasonality in the time-series, whereas the time-series from the tropical dry forests (green) show distinct seasonality that emanates from changes in the forest phenology. Boreal forests show strong seasonality caused by distinct freezing and thawing cycles within a year. The time-series is generated by aggregating a  $10 \times 10$  pixel area.

#### 2.4. Forest Land Use Change Detection

The general framework for near-real-time detection of forest land use change follows the methodology described in Mullissa et al. in 2023 [12]. We used the 2000 Hansen Global Forest Cover data with forest cover changes from 2000 to 2018 being removed [10] to define the stable forest baseline for 2018. The forest training samples were extracted from areas within the forest baseline, whereas the non-forest samples were extracted from areas outside the forest baseline. We used a machine learning model to derive the pixel-wise probability of forest land use change for every new incoming image starting on 1 January 2018 combined with the stable forest descriptor features discussed in the previous section.

In tropical humid and dry forests (i.e., in South American, Central American, African, Asian, Southeast Asian, and Oceania regions shown in Figure 3), we used a parametric probabilistic model described in [26] to separately derive the VV and VH polarization pixel-wise probability of forest land use change for every new incoming image starting 1 January 2018 combined with the stable forest descriptor features for the VV and VH polarizations discussed in the previous section. This model generates the pixel-wise non-forest probability by parameterizing the forest and non-forest probability density functions in a data-driven manner for every pixel within the forest baseline. We did not perform de-seasonalization on the Sentinel-1 SAR time series in tropical dry forests, as the backscattered signal decrease during forest disturbance is lower than the signal variation induced by change in the forest phenology due to seasonality [12]. Therefore, forest land use change detection was performed directly on the Sentinel-1 SAR ARD stack without a separate de-seasonalization step.

In the temperate and boreal forests (i.e., in North America, Europe, and Eurasia in Figure 4), there exists strong seasonality (Figure 3) that emanates from freezing in the winter months that decreases the forest backscatter intensity values approximately by 6 dB. This makes it very challenging to differentiate a frozen forest from a forest land use change. Therefore, in the preprocessing step, we filtered out images covered by snow or ice in the winter months as a quality assurance step. To detect forest land use change in the remaining images, we randomly generated 30,000 samples from forests within the boundary of the forest baseline and 30,000 samples for the non-forest class from outside the forest baseline to train a separate random forest model [27] for the VV and VH polarization to obtain pixel

wise forest land use change probability. These samples were evenly distributed over North America, Europe, and Eurasia. Visual quality assurance was applied to these samples to maintain the quality of the training data. We trained the random forest model using 30 trees and a bag fraction of 0.5.

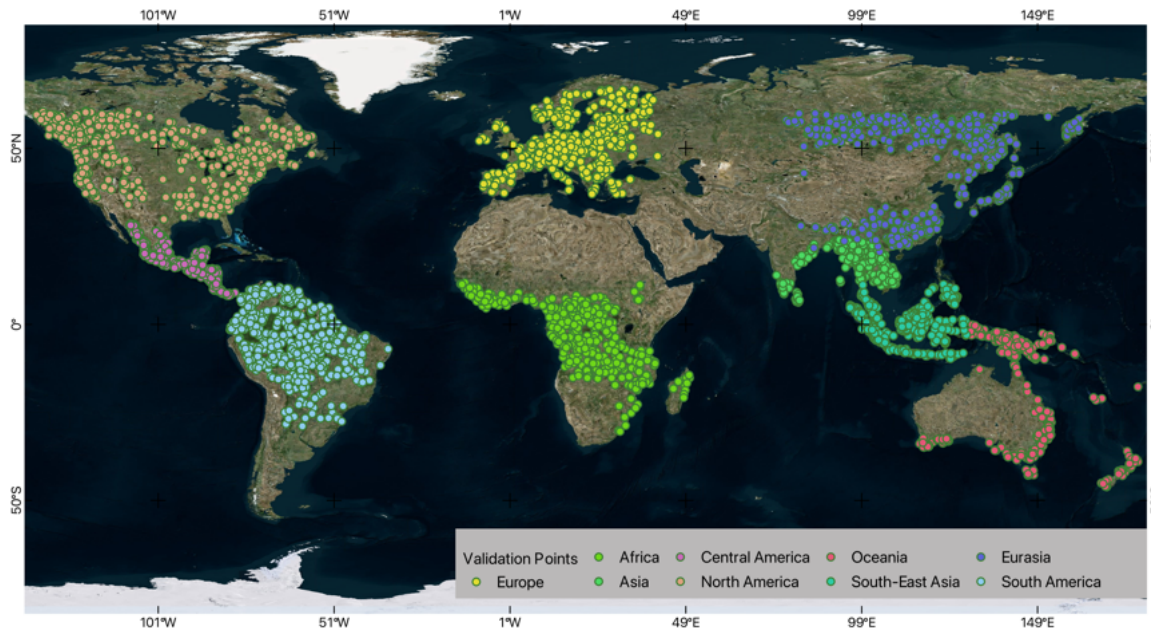


**Figure 3.** Validation reference sample locations for different sampling regions.

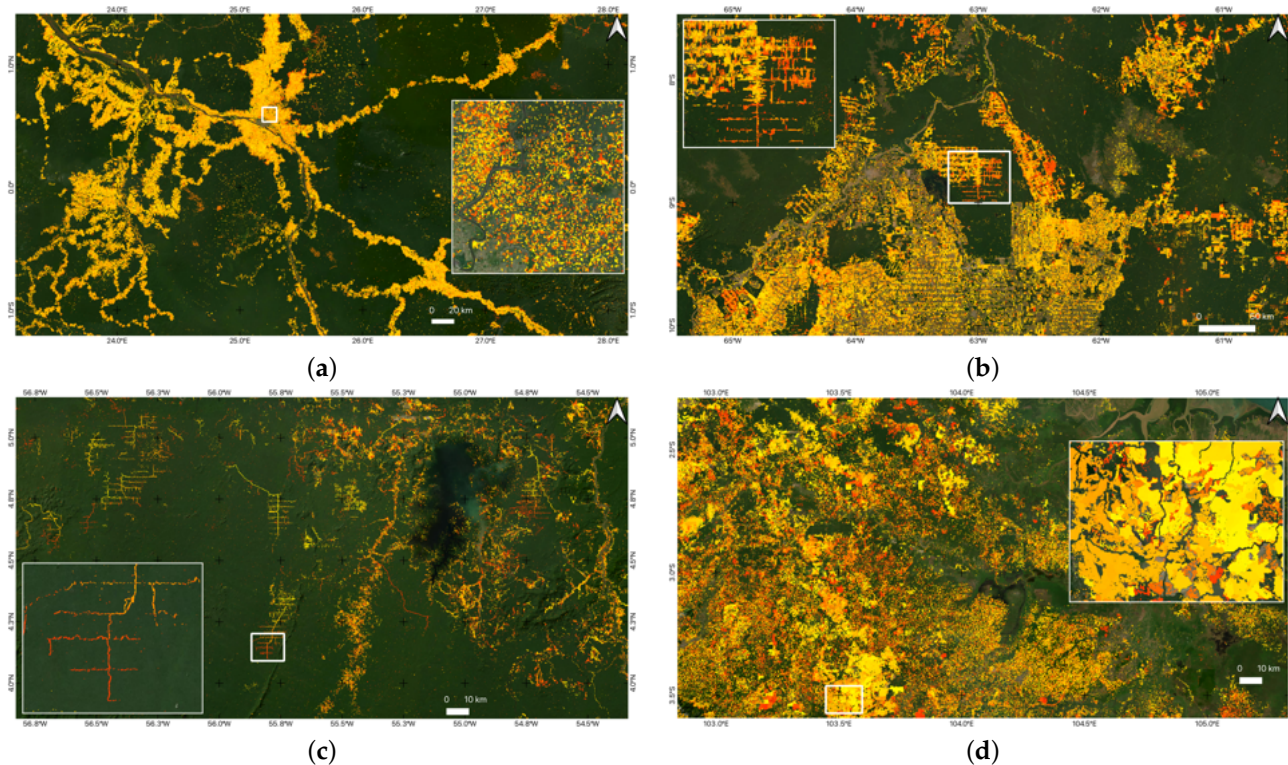


**Figure 4.** Cont.

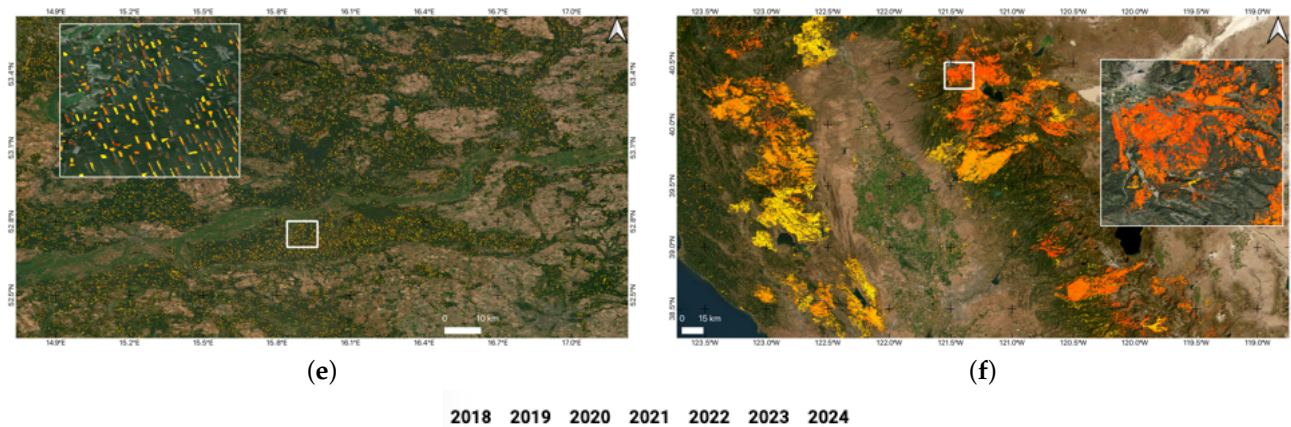


**Figure 4.** Forest land use changes and activities detected by LUCA. (a) Small-holder-agriculture-driven deforestation around the city of Kisangani in the Congo basin. (b) Agriculture-driven deforestation in Brazil. (c) Logging road development and selective logging in Suriname. (d) Large-scale commodity-driven deforestation in Indonesia. (e) Land use activity due to logging in a managed forest in Poland. (f) Land use activity induced by wildfires in California, USA. The background image was extracted from Google Earth.

We fused the forest land use change probability derived from the machine learning models in the VV and VH polarization in all forest biomes with an AND condition [12] to derive the forest land use change probability. From this, we derived forest land use change alerts by following the Bayesian updating approach detailed in [12,28]. We used a forest land use change probability threshold of 0.6 to flag potential forest changes and a posterior probability threshold of 0.8 to detect the changes in high confidence. We used a 90-day interval to change the flagged potential changes to a high confidence alerts. Alerts failing to reach these thresholds within the 90 days were discarded. Finally, we post-processed the detected alerts into a minimum mapping unit of 0.05 ha by discarding detections that were smaller than 5 pixels (8 interconnected). This helped remove clutter from the detected alerts maintaining a granular appearance in the forest land use change alert product.

## 2.5. Validation

We assessed the accuracy of the generated alerts from 2018 to 2024 by using area-adjusted accuracy assessment as suggested in Olofsson et al. in 2014 [29] and Olofsson et al. in 2020 [30]. These alerts were generated in an emulated near-real-time mode similar to other studies conducted in detecting near-real-time forest disturbance alerts [8]. We generated 450 samples in three strata using stratified random sampling in each geographic region of the world (Figure 3). These corresponded with South America, Central America, North America, Europe, Asia, Southeast Asia, Oceania, and Eurasia. We derived 150 random samples from the forest land use change strata and 300 random samples from the forest baseline and buffer area within a 200 m distance from alert pixels. The buffer areas were sampled to target the omission errors that occur in the proximity of detected forest land use changes. In the tropics, the reference labels were extracted visually from NICFI Planet monthly mosaic images. Whereas, we used National Agriculture Imagery Program (NAIP) aerial ortho-images to extract the reference labels for North America and cloud-free Sentinel-2 multispectral images to collect reference labels for Europe and Eurasia.

The bench mark forest cover map for 2018 was generated from the Landsat-based Hansen annual tree cover product [10], with forest cover changes before 2018 being removed using the forest cover loss layer in the same product. Some forest change events that happened before 2018 but were not included in the forest baseline dataset were detected by LUCA as new alerts in 2018. These events being actual alerts were not considered as

a commission error but were removed from the accuracy assessment sampling. Samples extracted from boundary pixels of large disturbance detections that were clearly shown in the higher resolution planet images were also discounted as commission errors.

We applied area weighting to the accuracy assessment to account for an unequal inclusion of probabilities, as the stratified sampling selected random samples that were substantially smaller than what were available in the detected alerts or forest cover baselines. The sample inclusion probabilities were generated based on the number of sample points and strata area. The inverse of the sample inclusion weights was used to construct an area-adjusted confusion matrix to compute the users' and producers' accuracy [31].

We applied temporal accuracy assessment to evaluate the timeliness of forest land use change detections. For this, we only selected samples that were verified as forest land use changes. The temporal accuracy was estimated by deriving the mean time lag (MTL) between the date the forest land use change was first observed in the reference image and the date LUCA first detected the forest land use change. Since the exact occurrence date of the forest land use change is not known, we adjusted the reference dates based on the time interval between the first image that showed the change and the previous image that showed no change [26], and we indicated the uncertainty due to the date adjustment.

### 3. Results

#### 3.1. Forest Land Use Change Alerts

Forest land use change alerts for all forest biomes are provided through a Google Earth Engine app (<https://ctrees.org/products/lua/map>, accessed on: 5 January 2024). We delivered the date the Sentinel-1-based forest land use change alert was detected for each 10 m pixel that falls within the boundary of the 2018 forest cover baseline. A few examples of the detected forest land use changes and activities for a variety of drivers is shown in (Figure 4).

We detected a total of 108.76 mha of forest land use change area globally from 2018 to 2024, with 25.92% detected from South America, 30.45% from Africa, 7.54% from Southeast Asia, 4.32% from Central America, 14.38% from Asia, 1.62% from Oceania, 7.56% from North America, 5.69% from Europe, and 2.46% from Eurasia. More than half of the total global deforestation was detected from South America and Africa. In these regions, small size changes (<1 ha) accounted for 14.14% and 23.73% of the total change detected in South America and Africa, respectively. Whereas, medium-sized (1–5 ha) forest land use changes accounted for 16.09% and 25.52% and large changes (>5 ha) accounted for 69.77% and 47.74% in South America and Africa, respectively. The small-sized changes were driven by selective logging of commercially valuable trees for timber production and the roads constructed to access them. The medium and large sized land use changes were driven by agricultural expansions and large-scale logging. From these, some of the detected changes started as small-sized (<1 ha) events that expanded in area to be large-sized change mostly due to agricultural and logging expansion.

In the tropics, the detected tropical forest land use change revealed a distinct seasonality in deforestation corresponding with the dry and wet seasons in those regions. For example, in the Democratic Republic of Congo, there were two distinct wet seasons per year which showed decreased deforestation and two dry seasons with increased deforestation activity (Figure 5), whereas in Brazil, there was a single wet season when deforestation subsided and a single dry season when deforestation increased. In Indonesia, the deforestation increase in 2018 and 2019 was linked to the dry season, with deforestation generally subsiding after 2020. Deforestation rates subside in most part of the tropics during the wet seasons due to difficulties in accessing the forests making logging activities more challenging [32].

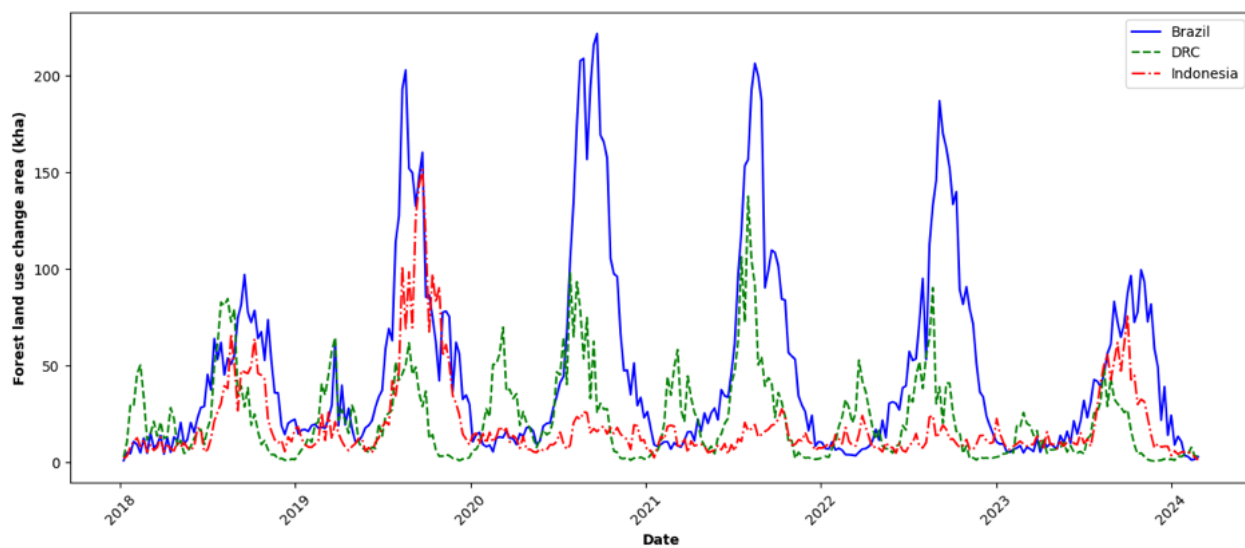


**Figure 5.** Seasonality of the forest land use changes detected from LUCA in Brazil, Democratic Republic of Congo, and Indonesia.

### 3.2. Validation Results

The accuracy assessment yielded high results in all continents Table 1. The alerts in general had low commission error (1–user accuracy), a higher omission error (1–producer accuracy) compared to the commission error, and a relatively low time lag between detection of changes with the actual date of change. The continents containing tropical humid and dry forests (i.e., Africa, Southeast Asia, Asia, Central America and South America) achieved the highest user and producer accuracy, suggesting accurate detection of forest land use changes with areas equivalent to the minimum mapping unit or larger.

**Table 1.** User and producer accuracy and adjusted mean time lag (MTL) for the LUCA alerts from 1 January 2018 to 15 January 2024 from the respective sampled regions shown in Figure 3.

Region	User Accuracy	Producer Accuracy	Adjusted MTL (Days)
North America	0.84	0.53	$235.12 \pm 7.5$ (90%)
Central America	0.87	0.62	$68.75 \pm 7.5$ (95%)
South America	0.83	0.78	$71.1 \pm 7.5$ (95%)
Africa	0.83	0.69	$48.8 \pm 7.5$ (95%)
Southeast Asia	0.83	0.76	$39.6 \pm 7.5$ (95%)
Asia	0.81	0.83	$50.5 \pm 7.5$ (95%)
Oceania	0.93	0.56	$56.16 \pm 7.5$ (95%)
Europe	0.78	0.40	$133.04 \pm 7.5$ (90%)
Eurasia	0.73	0.53	$139.79 \pm 7.5$ (90%)

The temperate region had more omission error due to the modality of forest land use activity that involved partial clearing after logging, which exacerbated omission error in these regions. The boreal forests especially in the northern part of Alaska, Finland, and Siberia contained more commission error induced by the remaining snow covered forest canopies, which were falsely detected as a forest land use change.

Analyzing alert events that were identified as commission errors, we identified two main sources of commission error. These were errors in the forest baseline layer that was used to make the alerts and seasonal flooding. In the case of omission errors, we identified three main sources of omission errors. The first source being the small changes in the backscattered radar signal that results from thinning of forest canopy, disturbance events with undamaged under-story caused by fire, etc., which did not allow for detection with high confidence. The second source of omission errors was backscattered radar signal

intensity from incomplete clearing of deforested plots closely resembling an intact forest; therefore, the computed forest land use change probabilities did not exceed the detection threshold. The third source of omission was an increase in moisture due to precipitation after the forest land use change events that increased the radar backscatter intensity to the pre-change level.

The estimated MTL of forest land use change varied in different regions. The tropical regions generally showed lower MTL values (Table 1) than did the temperate and boreal regions. In all regions, clear cut deforestation events were detected within  $\approx 20$  days, whereas changes related to incomplete clearing and degradation events took longer to be detected, thereby increasing the reported MTL values. Furthermore, in boreal forests, the snow cover images that were discarded further increased the MTL values for these regions, as no forest land use change detection took place within the freezing period, which generally lasted for months (Table 1).

### 3.3. Comparison with Other Forest Disturbance Alert Products

To evaluate the performance of LUCA in the tropics, we compared it with the RADD [8] and GLAD [32] forest disturbance alerts and the Hansen global forest loss dataset [10]. The good performance of the LUCA alert was clearly demonstrated in different forest biomes under a variety of forest land use change drivers (Figures 6 and 7). In the humid tropics, LUCA was effective in detecting forest land use changes relating to clear cut deforestation (Figure 6a,e,i,m) associated with logging and agricultural expansions, whereas the RADD alerts [8] was more effective in detecting the degradation related to selective logging and logging road development. This was more evident in countries like Gabon, where logging is the primary driver of degradation and deforestation (Figure 6e,f).

To compare the performance of different alerts, we calculated the detected annual forest land use change area for the LUCA, RADD, and GLAD alerts and for the Hansen global forest loss dataset in the Democratic republic of Congo and Brazil from 2020 to 2023. LUCA (Figure 8) detected a significantly higher number of forest land use changes than did GLAD, further highlighting the importance of radar-based alerts in overcoming the pervasive cloud cover found in tropical regions. LUCA also detected higher deforestation rate than did RADD, indicating that LUCA's coverage of all forest biomes enables it to detect more forest land use change activities than do the existing alerts that focus only on primary humid forests.

Comparing the effectiveness of the alerts in early detection of forest land use changes, we randomly selected 20 change events in 2021 to visually compare the day the changes were first detected. LUCA detected change events on average 10 days later than did the RADD alerts and 43 days earlier than did the GLAD alerts. For clear cut deforestation, both LUCA and RADD detected forest land use change events on the same dates, and the main difference was observed on the detection of forest degradation events such as selective logging. The GLAD alerts detected change events much later than did the LUCA and RADD alerts, indicating cloud cover plays a significant role in the late detection or omission of alerts.

Outside of the humid tropics, we compared LUCA with the Hansen global forest loss dataset for cumulative disturbance in 2021 [10], as both the RADD and GLAD alerts do not cover these regions. In this regard, LUCA clearly detected forest land use changes with different drivers. These ranged from large-area-agriculture and cattle-ranging-driven forest land use changes in Paraguay to small-scale-agriculture-driven events and logging activities in Myanmar Figure 7a,c. In temperate and boreal forests, LUCA also detected a variety of logging activities in managed forests in Georgia, USA, and Sweden Figure 7e–h. As shown in Figure 7, LUCA clearly revealed the extent of forest land use conversion and land use activities in these regions.

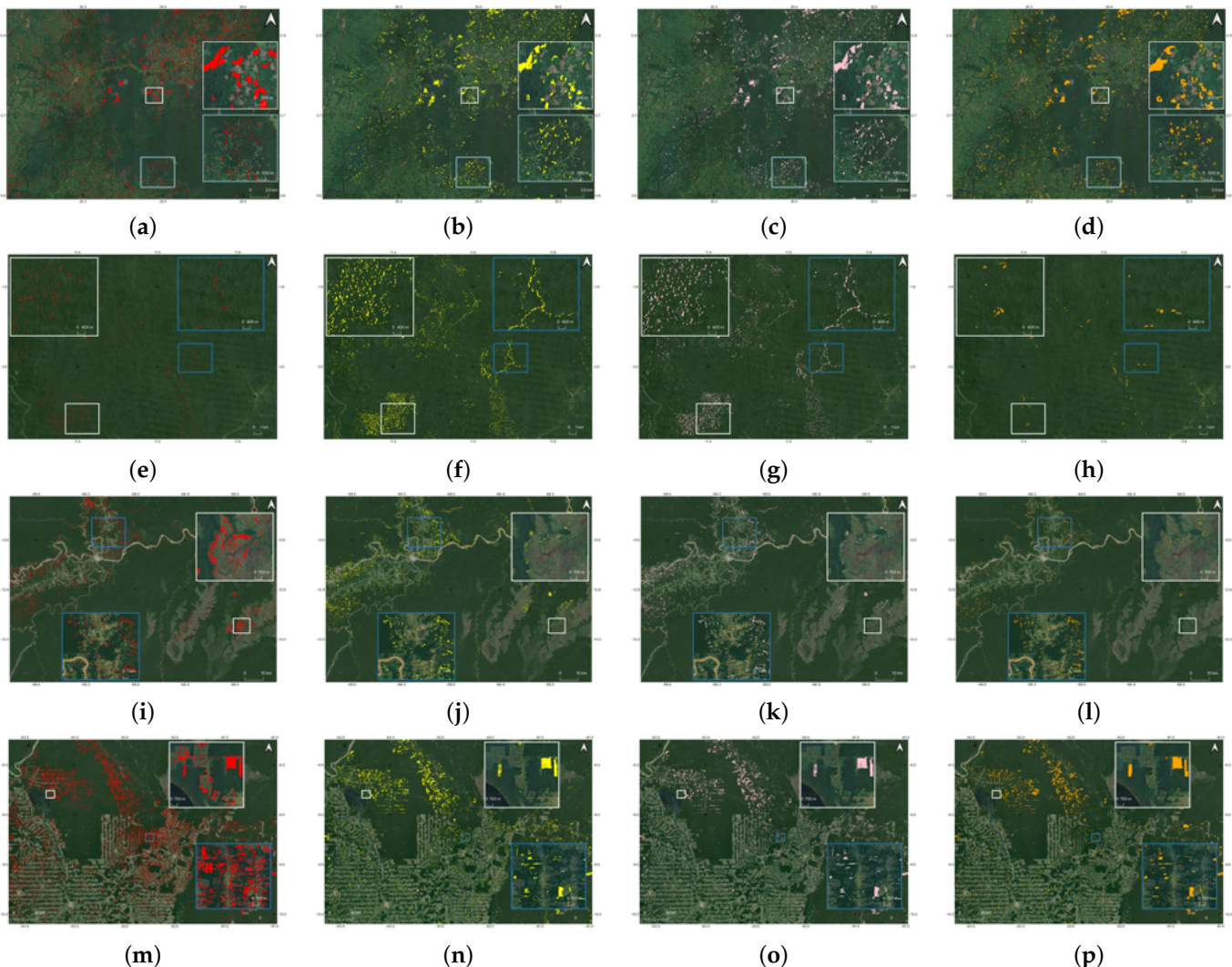


**Figure 6.** Cumulative forest land use change detection comparison between the LUCA (this study, on the left column), RADD [8] (second from the left column), and GLAD [32] (second from the right column) alert datasets and the Hansen global forest loss data [10] (right column) in 2021. (a–d) Small-holder-agriculture-driven deforestation. (e–h) Selective logging and logging road development. (i–l). Logging expansion (m–p). Large-scale-agriculture-driven deforestation. The background image was extracted from Google Earth.

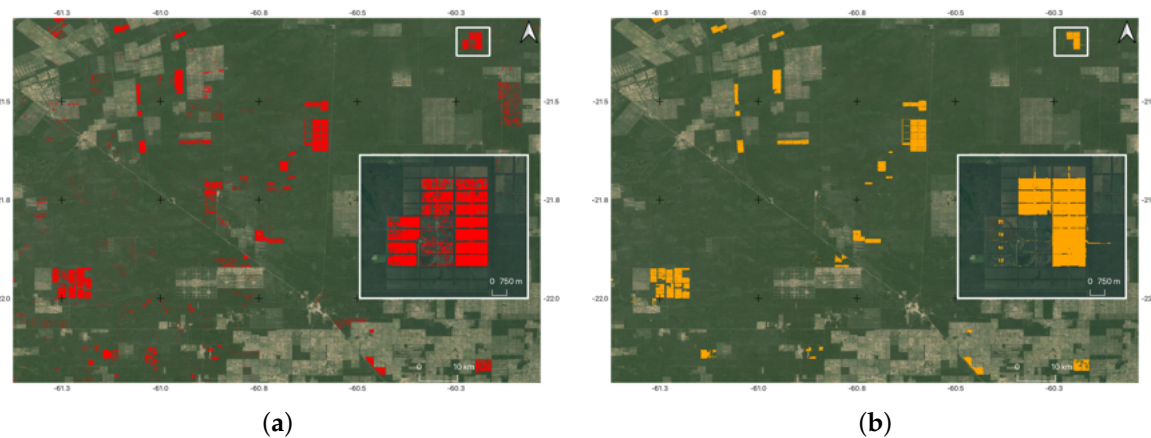


**Figure 7. Cont.**

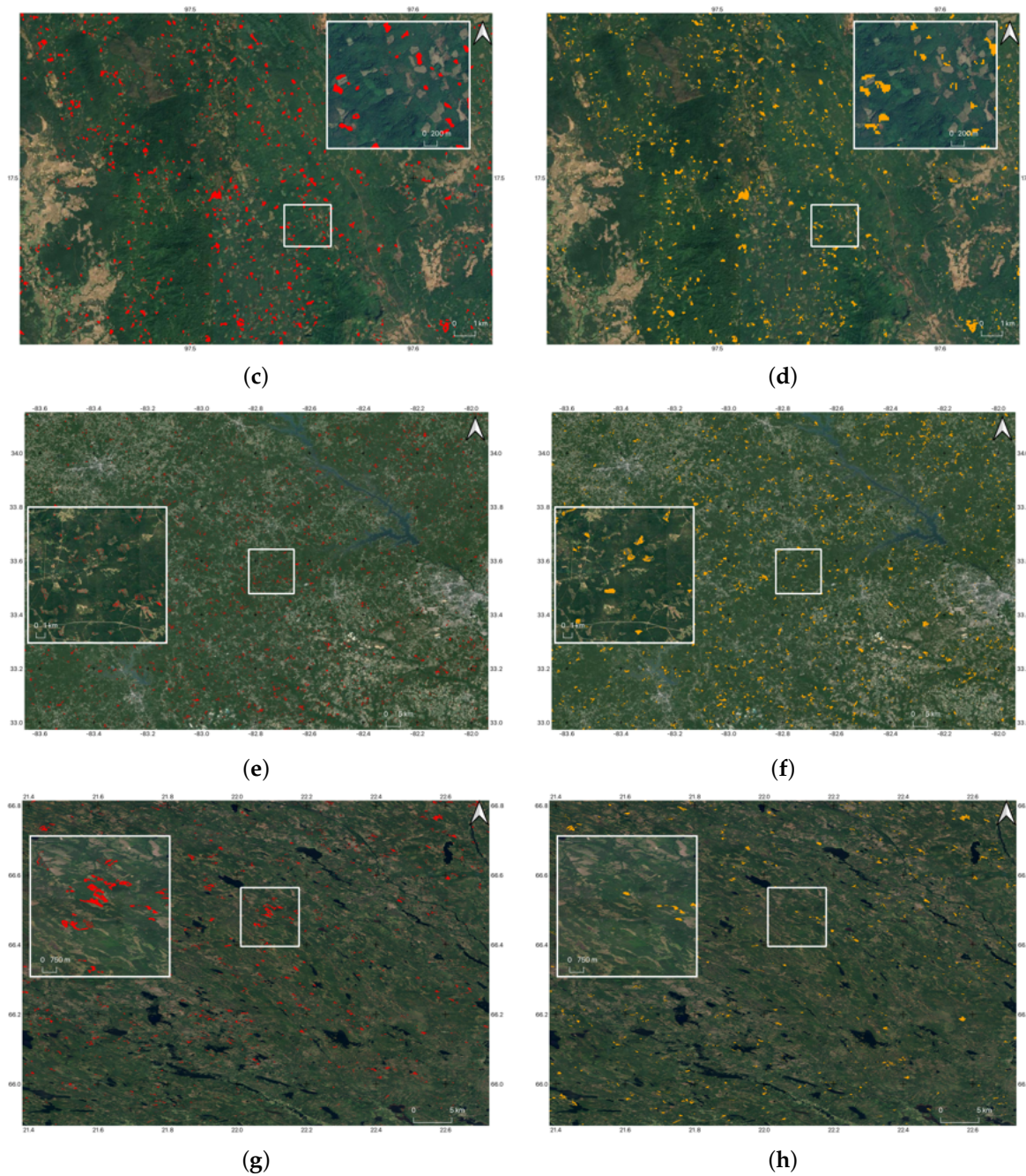


**Figure 7.** Cumulative forest land use change detection comparison between LUCA (this study, on the left column) and the Hansen forest cover loss dataset [10] (right column) in 2021. **(a,b)** Large-scale-commodity-agriculture-driven deforestation in Paraguay **(c,d)**. Small-holder-agriculture-driven deforestation in Myanmar **(e,f)**. Logging activity in a plantation forest in Georgia, USA **(g,h)**. Logging activity in boreal forests in Sweden. The background image was extracted from Google Earth.

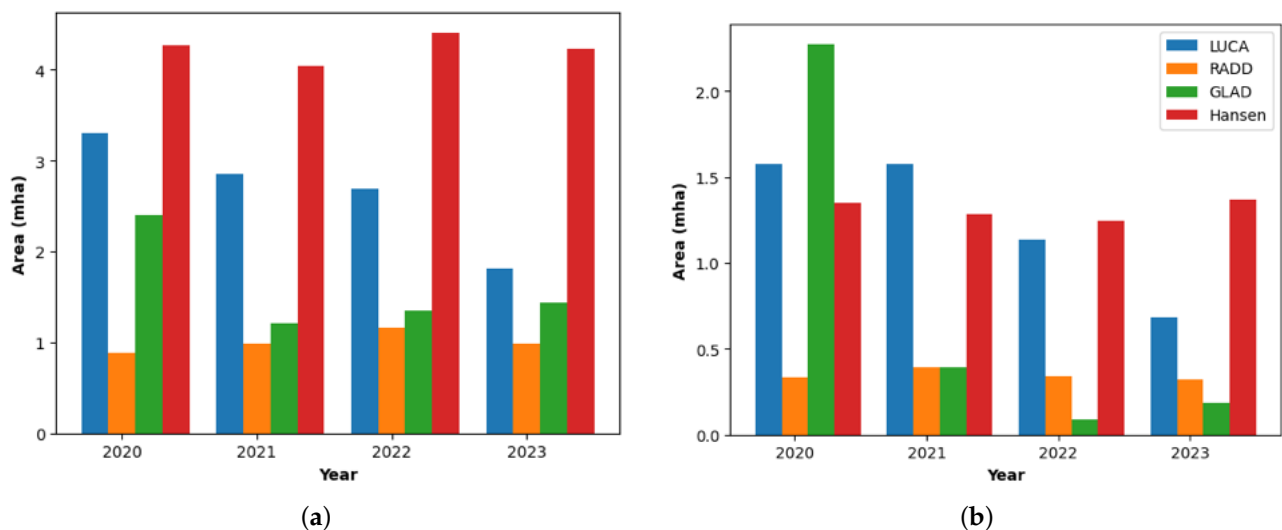


**Figure 8.** Comparison of detected forest land use change areas from 2020 to 2023 between LUCA (this study), RADD alerts [8], GLAD alerts [32], and the Hansen global forest loss data [10] in (a) Brazil and (b) the Democratic Republic of Congo. Area is reported in millions of hectares.

#### 4. Discussion

LUCA provided forest land use change alerts in unprecedented detail globally and in all forest biomes at a high accuracy. LUCA's forest definition at 15% tree cover density enabled alerts to be detected in areas that are not normally monitored by existing forest cover change alerts. The key advantage of LUCA is the near-real-time detection of forest land use changes in all biomes that existing alerts clearly did not provide. The Hansen global forest loss dataset operates in all forest biomes; however, the detected changes are cumulatively reported for the whole year, which does not allow for the near-real-time component in the detection. This property is clearly seen in detection's that were omitted in one year that were subsequently detected in the following year.

We selected a 15% threshold to minimize commission errors in the alerts by excluding large areas of non-forest covers, especially around the edge of forests, in savanna and woodland areas, and in urban areas. Furthermore, the Landsat 10% tree cover threshold includes large areas of crops and home gardens and shrub-dominated areas in savanna and dry or grassland areas. As a result, the confidence level for selecting the 10% threshold of tree cover for 30 m Landsat pixels is very low. The selection of a 15% forest density threshold to synthesize the forest baseline minimized the commission errors introduced within the alerts.

Generally, the LUCA alerts had a high user accuracy, indicating low commission errors in all biomes. This can be attributed to the probability fusion module implemented for both the VV and VH polarization that determines that forest land use change events that are detected should have high probability in both VV and VH polarizations. Therefore, it was effective in detecting deforestation involving complete clearing of an area. In regions involving tropical forest degradation and logging, it had a higher omission error compared to other radar alerts such as the RADD alerts. This omission was caused by a combination of factors relating to the partial clearing of trees during logging, systematic thinning of a forest cover during logging, and increased moisture in the ground after deforestation that raised the backscattered signal intensity to pre-deforestation levels. The stringent requirement for LUCA to detect alerts in both VV and VH polarization to have high confidence in the detected alerts also contributed to the omission errors detected in the accuracy assessment. The low minimum mapping unit (0.05 ha) in the alerts enabled LUCA to detect more forest land use changes compared to other near-real-time forest disturbance alert products.

LUCA provided forest land use change alerts in unprecedented detail and accuracy globally (Figure 4); however, some limitations resulting from the implemented radiometric

terrain correction and shadow-masking algorithm could be readily observed in mountainous regions in the Andes and Alps, which were displayed as false detection's on the shadow side of mountains. The low commission error of LUCA makes it a valuable tool for policy and law enforcement. As most near-real-time forest change alerts are designed to alert for new forest changes, the area derived from these alerts data may not accurately show the actual forest disturbance area. However, the derived alert areas can provide a valuable insight into the spatial and temporal trends. In this regard, the comparison with different near-real-time alerts provided a clear insight in the detection and reporting capability of LUCA (Figure 8).

Using the LUCA near-real-time forest land use change alerts, researchers could describe the spatial distribution of forest land use conversions with the time the conversion was first detected. The dense temporal cadence of the alerts further enables the usage of this data for law enforcement purposes to fight illegal deforestation. The existence of snow in the high latitudes decreases the capability of this product to detect forest land use changes in near-real-time, as most images are discarded in the winter season due to snow cover. Therefore, we advise caution when using the alerts in far northern latitudes. Finally, the generated forest land use change alerts do not contain attributions indicating drivers of forest change. The detected forest land use changes are mostly land use changes driven by human activities; however, some detected forest changes may constitute a land use activity without necessarily changing the land use from forest to non-forest (Figure 4e–f). Furthermore, the alerts do not differentiate between man-made land use activities and natural processes such as flooding, wind, and fire. Therefore, we advise caution when inferring deforestation and estimating area from this product. The area of forest land use change can be directly estimated from the visualization app using country-to-district level global administrative boundaries and custom user-defined areas provided to the system by the user in GeoJSON text format. This feature improves the usability of the data for users without a GIS background.

## 5. Conclusions

In this work, we developed global near-real-time forest land use change alerts based on Sentinel-1 SAR and machine learning, at a 10 m pixel size and a 0.05 ha minimum mapping unit. This product detects forest land use changes in all forest biomes in unprecedented detail and accuracy. This openly accessible dataset is expected to allow for the rapid assessment of deforestation and degradation, estimation of emissions for carbon policies and market, and an understanding of the drivers of change and dynamics of forest ecosystems. In future, we will work to (1) incorporate L-band SAR images from the NISAR [33] mission that is planned to be launched in late 2024 to increase the near-real-time detection capability of the alerts, (2) improve the detection methodology to minimize the omission errors reported in this work, (3) improve the accuracy and forest extent definition of the forest baseline that is used to define forested areas in this work, and (4) incorporate an alert attribution to understand the drivers of forest land use change.

**Author Contributions:** Conceptualization and methodology, A.M. and S.S.; software A.M., N.P., T.E. and V.M.; validation, A.M., F.O., R.D., V.M., N.P., A.A. and D.M.; writing—original draft preparation, A.M.; editing, A.M., S.S., R.D. and T.E.; All authors have read and agreed to the published version of the manuscript.

**Funding:** This research received no external funding.

**Data Availability Statement:** The alert dataset can be visualized, area analysis performed, and extracted charts downloaded using the LUCA viewer app (<https://ctrees.org/products/luca/map>, accessed on: 5 January 2024). For users from the scientific community that want to download the underlying raster data, it would be made available upon reasonable request.

**Acknowledgments:** The authors acknowledge the Grantham and High Tide foundations for their generous gift to UCLA and grants to CTrees for bringing new science and technology to solve envi-

ronmental problems. We also thank the Google Earth Engine team for providing the computational and storage resources necessary for processing the Sentinel-1 images to create this data product.

**Conflicts of Interest:** The authors declare no conflicts of interest.

## References

1. Zu Ermgassen, E.K.; Bastos Lima, M.G.; Bellfield, H.; Dontenville, A.; Gardner, T.; Godar, J.; Heilmayr, R.; Indenbaum, R.; Dos Reis, T.N.; Ribeiro, V.; et al. Addressing indirect sourcing in zero deforestation commodity supply chains. *Sci. Adv.* **2022**, *8*, eabn3132.
2. Xu, L.; Saatchi, S.S.; Yang, Y.; Yu, Y.; Pongratz, J.; Bloom, A.A.; Bowman, K.; Worden, J.; Liu, J.; Yin, Y.; et al. Changes in global terrestrial live biomass over the 21st century. *Sci. Adv.* **2021**, *7*, eabe9829.
3. Seymour, F.; Harris, N.L. Reducing tropical deforestation. *Science* **2019**, *365*, 756–757.
4. Longo, M.; Saatchi, S.; Keller, M.; Bowman, K.; Ferraz, A.; Moorcroft, P.R.; Morton, D.C.; Bonal, D.; Brando, P.; Burban, B.; et al. Impacts of degradation on water, energy, and carbon cycling of the Amazon tropical forests. *J. Geophys. Res. Biogeosci.* **2020**, *125*, e2020JG005677.
5. Dimitrov, R.S. The Paris agreement on climate change: Behind closed doors. *Glob. Environ. Politics* **2016**, *16*, 1–11.
6. Austin, K.G.; Heilmayr, R.; Benedict, J.J.; Burns, D.N.; Eggen, M.; Grantham, H.; Greenbury, A.; Hill, J.K.; Jenkins, C.N.; Luskin, M.S.; et al. Mapping and monitoring zero-deforestation commitments. *BioScience* **2021**, *71*, 1079–1090.
7. Lambin, E.F.; Furumo, P.R. Deforestation-Free Commodity Supply Chains: Myth or Reality? *Annu. Rev. Environ. Resour.* **2023**, *48*, 237–261.
8. Reiche, J.; Mullissa, A.; Slagter, B.; Gou, Y.; Tsendlbazar, N.E.; Odongo-Braun, C.; Vollrath, A.; Weisse, M.J.; Stolle, F.; Pickens, A.; et al. Forest disturbance alerts for the Congo Basin using Sentinel-1. *Environ. Res. Lett.* **2021**, *16*, 024005.
9. Slagter, B.; Reiche, J.; Marcos, D.; Mullissa, A.; Lossou, E.; Peña-Claros, M.; Herold, M. Monitoring direct drivers of small-scale tropical forest disturbance in near real-time with Sentinel-1 and-2 data. *Remote Sens. Environ.* **2023**, *295*, 113655.
10. Hansen, M.C.; Potapov, P.V.; Moore, R.; Hancher, M.; Turubanova, S.A.; Tyukavina, A.; Thau, D.; Stehman, S.V.; Goetz, S.J.; Loveland, T.R.; et al. High-resolution global maps of 21st-century forest cover change. *Science* **2013**, *342*, 850–853.
11. Diniz, C.G.; de Almeida Souza, A.A.; Santos, D.C.; Dias, M.C.; Da Luz, N.C.; De Moraes, D.R.V.; Maia, J.S.; Gomes, A.R.; da Silva Narvaez, I.; Valeriano, D.M.; et al. DETER-B: The new Amazon near real-time deforestation detection system. *IEEE J. Sel. Top. Appl. Earth Obs. Remote Sens.* **2015**, *8*, 3619–3628.
12. Mullissa, A.; Reiche, J.; Herold, M. Deep learning and automatic reference label harvesting for Sentinel-1 SAR-based rapid tropical dry forest disturbance mapping. *Remote Sens. Environ.* **2023**, *298*, 113799.
13. Rose, R.A.; Byler, D.; Eastman, J.R.; Fleishman, E.; Geller, G.; Goetz, S.; Guild, L.; Hamilton, H.; Hansen, M.; Headley, R.; others. Ten ways remote sensing can contribute to conservation. *Conserv. Biol.* **2015**, *29*, 350–359.
14. Shimabukuro, Y.E.; Santos, J.; Formaggio, A.; Duarte, V.; Rudorff, B.; Achard, F.; Hansen, M. The Brazilian Amazon monitoring program: PRODES and DETER projects. In *Global Forest Monitoring from Earth Observation*; CRC Press—Taylor & Francis Group: Boca Raton, FL, USA, 2012; Volume 2012, pp. 153–169.
15. Watch, G.F. *Global Forest Watch*; World Resources Institute: Washington, DC, USA, 2002. Available online: <http://www.globalforestwatch.org> (accessed on 5 January 2024).
16. Bouvet, A.; Mermoz, S.; Ballère, M.; Koleck, T.; Le Toan, T. Use of the SAR shadowing effect for deforestation detection with Sentinel-1 time series. *Remote Sens.* **2018**, *10*, 1250.
17. Doblas, J.; Reis, M.S.; Belluzzo, A.P.; Quadros, C.B.; Moraes, D.R.; Almeida, C.A.; Maurano, L.E.; Carvalho, A.F.; Sant’Anna, S.J.; Shimabukuro, Y.E. DETER-R: An operational near-real time tropical forest disturbance warning system based on Sentinel-1 time series analysis. *Remote Sens.* **2022**, *14*, 3658.
18. Watanabe, M.; Koyama, C.; Hayashi, M.; Kaneko, Y.; Shimada, M. Development of early-stage deforestation detection algorithm (advanced) with PALSAR-2/ScanSAR for JICA-JAXA program (JJ-FAST). In Proceedings of the 2017 IEEE International Geoscience and Remote Sensing Symposium (IGARSS), Fort Worth, TX, USA, 23–28 July 2017; pp. 2446–2449.
19. Gorelick, N.; Hancher, M.; Dixon, M.; Ilyushchenko, S.; Thau, D.; Moore, R. Google Earth Engine: Planetary-scale geospatial analysis for everyone. *Remote Sens. Environ.* **2017**, *202*, 18–27.
20. Mullissa, A.; Vollrath, A.; Odongo-Braun, C.; Slagter, B.; Balling, J.; Gou, Y.; Gorelick, N.; Reiche, J. Sentinel-1 SAR Backscatter Analysis Ready Data Preparation in Google Earth Engine. *Remote Sens.* **2021**, *13*, 1954.
21. Torres, R.; Snoeijs, P.; Geudtner, D.; Bibby, D.; Davidson, M.; Attema, E.; Potin, P.; Rommen, B.; Flory, N.; Brown, M.; et al. GMES Sentinel-1 mission. *Remote Sens. Environ.* **2012**, *120*, 9–24.
22. Hampel, F.R. The influence curve and its role in robust estimation. *J. Am. Stat. Assoc.* **1974**, *69*, 383–393.
23. Vollrath, A.; Mullissa, A.; Reiche, J. Angular-based radiometric slope correction for Sentinel-1 on google earth engine. *Remote Sens.* **2020**, *12*, 1867.
24. Hoekman, D.H.; Reiche, J. Multi-model radiometric slope correction of SAR images of complex terrain using a two-stage semi-empirical approach. *Remote Sens. Environ.* **2015**, *156*, 1–10.
25. Quegan, S.; Yu, J.J. Filtering of multichannel SAR images. *IEEE Trans. Geosci. Remote Sens.* **2001**, *39*, 2373–2379.

26. Reiche, J.; Verhoeven, R.; Verbesselt, J.; Hamunyela, E.; Wielaard, N.; Herold, M. Characterizing tropical forest cover loss using dense Sentinel-1 data and active fire alerts. *Remote Sens.* **2018**, *10*, 777.
27. Pal, M. Random forest classifier for remote sensing classification. *Int. J. Remote Sens.* **2005**, *26*, 217–222.
28. Reiche, J.; De Bruin, S.; Hoekman, D.; Verbesselt, J.; Herold, M. A Bayesian approach to combine Landsat and ALOS PALSAR time series for near real-time deforestation detection. *Remote Sens.* **2015**, *7*, 4973–4996.
29. Olofsson, P.; Foody, G.M.; Herold, M.; Stehman, S.V.; Woodcock, C.E.; Wulder, M.A. Good practices for estimating area and assessing accuracy of land change. *Remote Sens. Environ.* **2014**, *148*, 42–57.
30. Olofsson, P.; Arévalo, P.; Espejo, A.B.; Green, C.; Lindquist, E.; McRoberts, R.E.; Sanz, M.J. Mitigating the effects of omission errors on area and area change estimates. *Remote Sens. Environ.* **2020**, *236*, 111492.
31. Stehman, S.V. Estimating area and map accuracy for stratified random sampling when the strata are different from the map classes. *Int. J. Remote Sens.* **2014**, *35*, 4923–4939.
32. Hansen, M.C.; Krylov, A.; Tyukavina, A.; Potapov, P.V.; Turubanova, S.; Zutta, B.; Ifo, S.; Margono, B.; Stolle, F.; Moore, R. Humid tropical forest disturbance alerts using Landsat data. *Environ. Res. Lett.* **2016**, *11*, 034008.
33. Kellogg, K.; Hoffman, P.; Standley, S.; Shaffer, S.; Rosen, P.; Edelstein, W.; Dunn, C.; Baker, C.; Barela, P.; Shen, Y.; others. NASA-ISRO synthetic aperture radar (NISAR) mission. In Proceedings of the 2020 IEEE Aerospace Conference, Big Sky, MT, USA, 7–14 March 2020; pp. 1–21.

**Disclaimer/Publisher’s Note:** The statements, opinions and data contained in all publications are solely those of the individual author(s) and contributor(s) and not of MDPI and/or the editor(s). MDPI and/or the editor(s) disclaim responsibility for any injury to people or property resulting from any ideas, methods, instructions or products referred to in the content.